

# Unsupervised clothing change adaptive person ReID

Ziyue Zhang, Shuai Jiang, Congzhentao Huang, Richard YiDa Xu

University of Technology Sydney

## Abstract

Clothing changes and lack of data labels are both crucial challenges in person ReID. For the former challenge, people may occur multiple times at different locations wearing different clothing. However, most of the current person ReID research works focus on the benchmarks in which a person’s clothing is kept the same all the time. For the last challenge, some researchers try to make model learn information from a labeled dataset as a source to an unlabeled dataset. Whereas purely unsupervised training is less used. In this paper, we aim to solve both problems at the same time. We design a novel unsupervised model, Sync-Person-Cloud ReID, to solve the unsupervised clothing change person ReID problem. We develop a purely unsupervised clothing change person ReID pipeline with person sync augmentation operation and same person feature restriction. The person sync augmentation is to supply additional same person resources. These same person’s resources can be used as part supervised input by same person feature restriction. The extensive experiments on clothing change ReID datasets show the out-performance of our methods.

## 1 Introduction

Person re-identification (ReID) (Ye et al. 2021) is designed to match specific pedestrians in images or video sequences. The main challenge of ReID is that the ReID features variations of the same person in different situations are usually significant because of viewpoint or situation differences, which makes it challenging to identify the same person. Meanwhile, the lack of ReID features variations of different people in the same situation or wearing the same clothing also influence ReID performance. Current works in person ReID are mostly to learn discriminative features of person identity by a specifically designed backbone model (Chang, Hospedales, and Xiang 2018; Wang et al. 2019a). There are also works focusing on problems of occlusions (Hou et al. 2019), different poses (Qian et al. 2018), illumination changes (Zhang et al. 2020) and resolution changes (Li et al. 2019).

The clothing change plays a crucial character in person ReID. However, the researchers assume the same person wears the same clothes, which means the above works cannot handle the clothing change variations in person ReID. In daily life, people usually change their clothes, which means

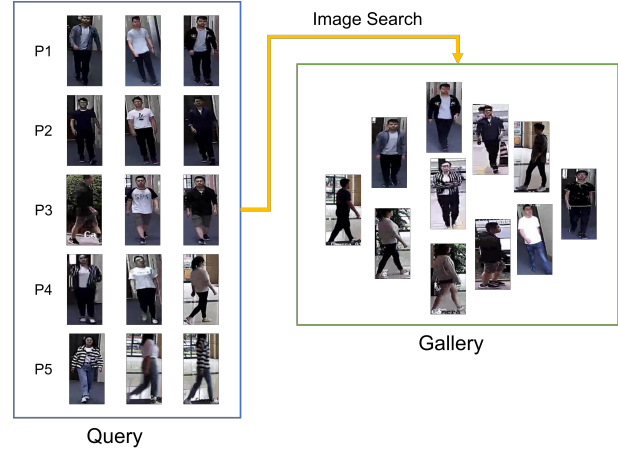


Figure 1: Example of clothing change person ReID dataset Real28 (Wan et al. 2020). The query images include five persons’ images. The images of each row in the query are from the same person with different clothes. The gallery images consist of different person images with different clothes.

that the same person captured by the camera at different times may wear different clothes. As shown in the figure 1, clothing change ReID datasets consist of a person with different clothing and researchers try to find the same person under such settings, which is more in line with the real-life scene. The existing conventional methods tend to fail in such a scenario because of the unreliability of clothing texture information and the lack of the same person’s ID information with different clothing.

Another key problem is that it is challenging to get person ReID labels. Because it is expensive to record person images across multiple cameras, many previous works try to address person ReID problem by unsupervised or semi-supervised learning (Lin et al. 2019; Yu et al. 2019; Wang et al. 2018b). Most of these methods use unsupervised domain adaptation. They first pretrain a model on the source labeled dataset and then fine-tune it on the target unlabeled dataset. However, these methods still need at least one label dataset and suffer from the variation between the source and target domain. Hence, we choose to use purely unsupervised learning for our method.

In this paper, we propose a pure unsupervised model called Sync-Person-Cloud ReID to solve the unsupervised clothing change person ReID problem. The whole pipeline follows the below procedure. The person image features of the training data are extracted by the CNN backbone. Then we use a clustering algorithm to cluster image features and produce pseudo labels. At last, the backbone is trained with a contrastive loss such as InfoNCE loss using the storage person image features. This pipeline can initially obtain pedestrian features by purely unsupervised learning. However, it is still not able to separate the noise information caused by different clothes and the unsupervised features are not robust enough. Because people always change clothes on daily life, it is not possible to create a simple disentanglement classifier. So to better bridge the gap between the same person features with different clothing and improve the unsupervised performance, we have added several innovations summarised as follows:

1. We use a clothing change person augmentation module to generate synthetic person images with different clothes. A person image is sent to the augmentation module to get multiple synthetic person images with person parsing and clothing template. By using this scheme, we can get semi-supervised information from synthetic images which can be seemed as the same person.
2. To constrain the synthetic same person features, we adopt a self cluster loss to reduce the distance between these features. This will let the later cluster algorithm perform better by constraining the same person images with different clothes as the same pseudo label. The augmentation images can use the semi-supervised information to make the ReID backbone more robust.
3. Both the average and batch hard sampling are used on the cluster image features. It takes much fewer GPU resources than using all image features. With the average sampling, the model can be trained by the whole dataset feature to get high performance on a whole large dataset. With batch hard sampling, the model can be trained faster and more accurately.

The rest of the article is organized as follows. Section **Related work** illustrates related works on conventional person Re-ID, unsupervised person ReID and clothing change person ReID. Section **Method** describes our pipeline structure for getting unsupervised clothing change person ReID features in detail. Our experiment results and details are shown in section **Experiments**. We finally conclude our work in section **Conclusion**.

## 2 Related work

### 2.1 Conventional Person ReID

Most researchers focused on traditional person ReID. In the early research, one primary method of person ReID is metric learning, which is to formalize the problem as supervised metric learning where a projection matrix is sought out (Yang, Wang, and Tao 2017; Yi et al. 2014; Ding et al. 2015). Benefiting from the advances of convolutional neural network (CNN) architectures, another primary method is to

learn appropriate features associated with the same ID using features distance information (Hermans, Beyer, and Leibe 2017) on a backbone module (Chang, Hospedales, and Xiang 2018; Si et al. 2018), such as Resnet50 (He et al. 2016). Our work can seem like the second one. We also use a modified Resnet50 as our ReID backbone.

After getting the ReID features, the person re-id is to train the backbone with contrastive loss. The contrastive loss is to reduce the distances between image features of the same person and to increase the distances between the image features of different persons. Several methods employed triplet loss (Hermans, Beyer, and Leibe 2017; Chen et al. 2017; Song et al. 2018) to constrain the distances between image triplets. Some researchers also use identity classification loss (Zheng, Zheng, and Yang 2017; Zhong et al. 2018) to make the ReID problem an image classification problem. Although these works focus on person ReID, they may fail in some circumstances, e.g., when person images are with different clothing. They cannot handle clothing change ReID data, which will lead to low performance.

### 2.2 Unsupervised Person ReID

Early unsupervised Re-ID works are mainly to learn invariant components, i.e., dictionary or metric, whose discriminability or scalability is relatively insufficient. For deeply unsupervised methods, there are two main types of methods.

The first is unsupervised domain adaptation (UDA), which transfers the knowledge on a labeled source dataset to the unlabeled target dataset. Due to the powerful supervision in the source dataset, it can learn enough information for person ReID. For example, (Deng et al. 2018) presents a baseline to translate the labeled images from source to target domain in an unsupervised manner with self-similarity and domain-dissimilarity. (Lin et al. 2018) developed a Multi-task Mid-level Feature Alignment network that can be jointly optimised under the person's identity classification and the attribute learning task with a cross-dataset mid-level feature alignment regularisation term. (Wang et al. 2018b) proposed a model named Transferable Joint Attribute-Identity Deep Learning for simultaneously learning an attribute-semantic and identity discriminative feature representation space transferable to any new target domain without the need for collecting new labeled training data from the target domain. Although these works can learn a new unlabeled dataset, the large domain shift is still a challenge for the UDA problem.

Another method is end-to-end purely unsupervised learning, which generally generates pseudo labels from the completely unlabeled data using a clustering algorithm. (Fan et al. 2018) proposed an effective baseline named the progressive unsupervised learning (PUL) method to transfer pretrained deep representations to unseen domains. (Fu et al. 2019) proposed a self-similarity grouping approach to get the pseudo identities by exploiting the potential similarity of unlabeled samples to build multiple clusters from different views automatically. (Lin et al. 2019) proposed a bottom-up clustering approach to jointly optimize a convolutional neural network and the relationship among the individual samples. (Dai et al. 2021) proposed a cluster contrast that stores

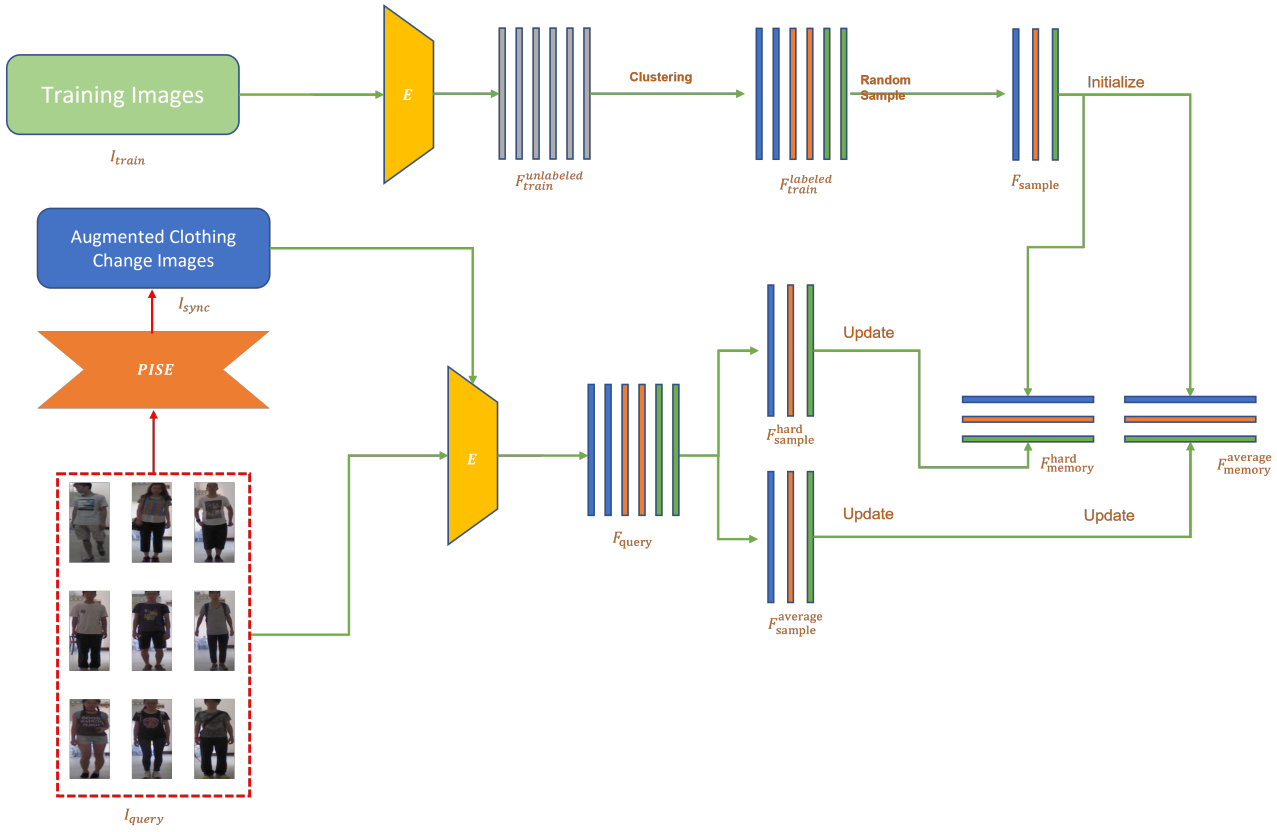


Figure 2: The whole pipeline of our unsupervised clothing change ReID model (best viewed in color). For conciseness, we do not show the augmentation module *PISE* details here.

feature vectors and computes contrast loss in the cluster level to solve the inconsistency problem for cluster feature representation.

In this paper, we choose to use end-to-end purely unsupervised learning as our initial pipeline.

### 2.3 Clothing Change Person ReID

In a practical surveillance scenario, there are a large number of persons with changing clothes. Some researchers use the face and body appearance as the supplement information to address clothing change ReID. (Xue et al. 2018) proposed a cloth-Clothing Change Aware Network to address the clothing change ReID by separately extracting the face and body context representation. However, the face and body appearance might be unavailable, which may cause the model to fail in some scenarios. The infrared or depth images can also be the supplement information to help address clothing change ReID (Barbosa et al. 2012; Wu et al. 2017). However, the depth information is only applicable in indoor environments, which is not suitable for all scenarios. And the information of the infrared image is much less than RGB images’, which makes the ReID less effective.

For purely RGB clothing change person ReID, the methods mostly work on reducing the domain gap between the image features of the same person with different clothes. (Hong et al. 2021) proposed a Fine-grained Shape-

Appearance Mutual learning framework that learns fine-grained discriminative body shape knowledge in a shaped stream and transfers it to an appearance stream to complement the cloth-unrelated knowledge in the appearance features. (Wan et al. 2020) proposed a new clothing change dataset with both real and synthetic images. (Shu et al. 2021) proposed a semantic-guided pixel sampling model to automatically learn cloth-irrelevant cues. (Yang, Wu, and Zheng 2019) proposed a new dataset and present a spatial polar transformation to learn cross-cloth invariant representation.

In this paper, we propose a clothing change augmentation and self identity image constrain to help our unsupervised model solve the clothing change ReID problem

### 2.4 Data Augmentation in Person ReID

Ordinary data augmentations such as random resizing, cropping, random erasing and horizontal flipping are widely used in Re-ID. Besides, using GAN to generates augmented images is also applied in some methods. (Zheng, Zheng, and Yang 2017) first attempted to use the GAN for person ReID. It improves the supervised feature representation learning with the generated person images. (Liu et al. 2018) introduced pose constraints to improve the quality of the generated person images, generating the different pose person images. (Zhong et al. 2018) add camera style information in the image generation process to address the cross cam-

era adaptation problem. Some works also use GAN to generate synthetic person images from one domain to another. (Wang et al. 2019b; Zhang et al. 2021b) used GAN to generate the same content person image from RGB modality to IR modality. (Wang et al. 2018c) use GAN to transfer low resolution images to high resolution versions.

In our work, we use a pretrained Decoupled GAN proposed by (Zhang et al. 2021a) to generate different clothes person images. These images are then seemed as same person images by the same person constrain loss.

### 3 Method

#### 3.1 Overview of Pipeline

To get the unsupervised clothing change person ReID feature, inspired by (Dai et al. 2021), we proposed our unsupervised pipeline for clothing change ReID in a similar way. We show our whole model pipeline in Figure 2.

First, we use a modified resnet-50 (He et al. 2016) as our backbone module  $E$  for ReID feature extraction, which is pretrained on ImageNet (Deng et al. 2009). All train dataset images  $I_{train}$  will be sent to  $E$  to get unlabeled training dataset ReID features  $F_{train}^{unlabeled}$ .

$$F_{train}^{unlabeled} = E(I_{train}) \quad (1)$$

Then, we use a clustering algorithm DBScan (Ester et al. 1996) to generate pseudo labels for each input image feature. DBScan is a density-based clustering method, whose clustering results almost independently depend on the sequence of nodes. It can discover the cluster of any shape and effectively discover noise points, which is more suitable in person ReID problem scenario than other clustering algorithms such as Kmeans (MacQueen et al. 1967) and agglomerative clustering (Day and Edelsbrunner 1984). DBScan requires two hyper-parameters. The first is the maximum distance  $\varepsilon$ , which represents the neighbor radius of the definition density. In other words,  $\varepsilon$  is the distance between two samples for one to be considered as in the neighborhood of the other. Another is the cluster neighbor density threshold  $M$ , which donates the minimum number of samples in a neighborhood for an instance to be considered as a core instance. We set  $\varepsilon$  to 0.4 and  $M$  to 4 in all our experiments. Through DBScan clustering, the cluster ID is assigned to each training image as the pseudo label to get the pseudo-labeled training dataset ReID features.

$$F_{train}^{labeled} = DBScan_{\varepsilon}^M(F_{train}^{unlabeled}). \quad (2)$$

Finally, a contrastive loss with the global and average sample is used to compute the loss values between the query instances and the memory dictionary. The details of the computation and other components will be illustrated later.

#### 3.2 Clothing Change Person Image Augmentation

To get the same person features with different clothes, we introduce a pretrained Person Image Synthesis module  $PISE$  (Zhang et al. 2021a) here.  $PISE$  is a two-stage generative model for Person Image Synthesis and Editing, which is able

to generate realistic person images with desired poses, textures, or semantic layouts. The effectiveness and function of  $PISE$  are shown in Figure 3.

We use  $PISE$  to get the synthetic person images  $I_{sync}$  from each input query image  $I_{query}$ .

$$I_{sync} = PISE(I_{query}). \quad (3)$$

We use  $S$  different clothing style template for each input query image to get the corresponding  $S$  synthetic images. In our settings,  $S$  is set to 4. These synthetic images can be assumed to have the same identity but different clothes.

#### 3.3 Cluster Contrast and Update Procedure

In the very first step of each epoch training, we random sample one single image feature from each clustered pseudo-labeled features  $F_{train}^{labeled}$  using uniform sample  $U$ .

$$F_{sample}(i) = U(F_{train}^{labeled}(i)). \quad (4)$$

We donate the  $N$  as the cluster number and  $F_{sample}(i)$  as a single feature from  $i_{th}$  cluster features  $F_{train}^{labeled}(i)$ . We use these sampled features as the initial memory features for  $F_{memory}^{average}$  and  $F_{memory}^{hard}$ .

During the model training stage, we set the number for query image  $I_{query}$  as  $P * K$ , in which  $P$  is person identity number and  $K$  is the instance number for each person identity. We send these  $K$  person images to the  $PISE$  module to get the corresponding  $S * K$  synthetic person images  $I_{sync}$  with different clothes for each query person. All these images are sent to the ReID backbone to get the query features  $F_{query}$ .

$$F_{query} = E(I_{query} \cup I_{sync}). \quad (5)$$

For updating the feature memory, inspired by (Concha et al. 2011) which handle the variant dimensions of probability features using normalization, we select the hardest instance and average instance for each person identity with momentum  $m$ . We maintain two features memory, which is

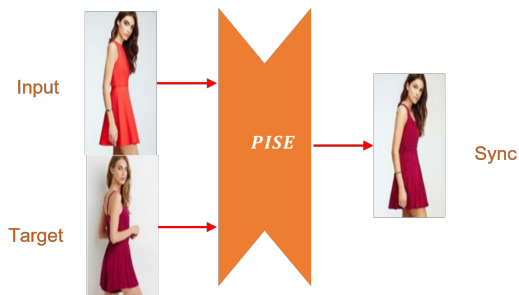


Figure 3: The function of the  $PISE$  module. It takes two inputs which are original input query person image and target clothing style image. It will generate a image with the same content of input query person image and same clothing style of input target clothing style image. The synthetic image can be assumed as the same person identity with original input query person image.

average feature memory  $F_{memory}^{average}$  and hardest feature memory  $F_{memory}^{hard}$ . For a certain cluster with person identity  $i$  in hardest feature memory  $F_{memory}^{hard}$ , its feature vector is updated by:

$$\begin{aligned} f_{query}^{hard} &= \arg \max_{f_{query}} KL(f_{query}, F_{memory}^{hard}(i)), \\ f_{query} &\in F_{query}(i), \\ F_{memory}^{hard}(i) &= m \cdot F_{memory}^{hard}(i) + (1 - m) \cdot f_{query}^{hard}, \end{aligned} \quad (6)$$

where the batch hard instance  $f_{query}^{hard}$  is the instance with the minimum similarity to the cluster feature. We measure the similarity with KL divergence.  $m$  is the momentum updating factor.  $F_{query}(i)$  is the instance features set with cluster ID  $i$  in the current mini batch.

For a certain cluster with person identity  $i$  in average feature memory  $F_{memory}^{average}$ , its feature vector is updated by:

$$\begin{aligned} f_{query}^{average} &= \frac{\sum f_{query}}{(S + 1) \times K}, \\ f_{query} &\in F_{query}(i), \\ F_{memory}^{average}(i) &= m \cdot F_{memory}^{average}(i) + (1 - m) \cdot f_{query}^{average}, \end{aligned} \quad (7)$$

where the batch hard instance  $f_{query}^{average}$  is the average instance of all query features  $F_{query}(i)$  from identity  $i$ .

The query image features (including the original input and synthetic image features) are compared to all cluster features (including average memory and hardest memory) with InfoNCE loss (Oord, Li, and Vinyals 2018). The InfoNCE loss can be formulated as follows:

$$\begin{aligned} L_q(F_{query}, F_{memory}) &= -\log \frac{\exp(f_q \cdot f_m^+) / \tau}{\sum_{i=0}^K \exp(f_q \cdot f_m(i)) / \tau}, \\ f_q &\in F_{query}, f_m \in F_{memory}^{hard} \cup F_{memory}^{average}. \end{aligned} \quad (8)$$

where  $f_m^+$  is the positive memory cluster feature vector to query instance  $f_q$ .  $\tau$  is a temperature hyper-parameter (Wu et al. 2018). The loss tries to classify  $f_q$  as  $f_m^+$  through low value when  $f_q$  is similar to its positive cluster feature and dissimilar to all other cluster features.

### 3.4 Self Identity Constrain

Since the synthetic clothing change images can seem as the same person, we use a self identity constrain loss to reduce the variance between all synthetic person image features generated from the same input person image. We define this loss as follows:

$$\begin{aligned} L_s &= \frac{\sum_{i=0}^P \sum_{j=0}^K \sum_{a,b=0}^{S+1} KL(f_{query}^a, f_{query}^b)}{P \times K \times (S + 1)}, \\ f_{query} &\in F_{query}. \end{aligned} \quad (9)$$

The loss tries to classify all synthetic and corresponding original input person image features as the same person by reducing the KL divergence between them.

---

### Algorithm 1: Whole training process for our method

---

**Require:** Unlabeled training images  $I_{train}$

**Require:** Backbone  $E$  Pretrained on Imagenet

**Require:** Pretrained clothing change person image synthesis module  $PISE$

**Require:** Hyper parameters  $P, K, S, m, \tau, M, \varepsilon$

- 1: **for**  $n \in [1, max\_epochs]$  **do**
  - 2:   Send  $I_{train}$  to  $E$  to get all features  $F_{train}^{unlabeled}$ .
  - 3:   Cluster  $F_{train}^{unlabeled}$  to get  $F_{train}^{labeled}$  using Eq.2.
  - 4:   Initialize the memory  $F_{memory}^{average}$  and  $F_{memory}^{hard}$  with  $F_{sample}$  using Eq.4.
  - 5:   **for**  $i \in [1, max\_iter]$  **do**
  - 6:     Sample  $P \times K$  person images  $I_{query}$  from  $I_{train}$
  - 7:     Sent  $I_{query}$  to  $PISE$  to get  $I_{sync}$  using Eq.3.
  - 8:     Sent  $I_{query}$  and  $I_{sync}$  to  $E$  to get query features  $F_{query}$  using Eq.5.
  - 9:     Compute InfoNCE loss and self identity loss using Eq.8 and Eq.9 and compute the total loss  $L = L_q + \alpha L_s$ .
  - 10:    Backwards the total loss functions to optimize our encoder  $E$ .
  - 11:    Update hardest memory and average memory using Eq.6 and Eq.7.
  - 12:   **end for**
  - 13: **end for**
- 

## 3.5 Whole Train Process

We show our whole unsupervised training process in Algorithm 1. As shown in the pseudo code, the entire training process of each epoch consists of three stages, which are 1) cloud for pseudo label and memory initialization, 2) loss computation for updating backbone and 3) memory update.

## 4 Experiments

### 4.1 Implementation Details

We implement our model with Pytorch ((Paszke et al. 2019)). We conduct our model based on the unsupervised learning baseline (Dai et al. 2021). We adopt the ResNet-50 ((He et al. 2016)) as our backbone. We modify the last layer stride to be 1 in the backbone Resnet50 to make final output features have more abundant information. Then we extract 2048d features for all images from the GAP layer in our backbone. During testing, we take the 2048d features to calculate the distance. For the beginning of each epoch, we use DBScan as our clustering method to generate pseudo labels for unlabeled input images.

The input image is resized to  $256 \times 128$ . The random cropping and horizontal flipping are performed as the augmentation methods. We haven't used random erasing and image padding because we want to keep the content of the input image to get synthetic clothing change person images. The batch size  $P \times K$  is set as 32, in which  $K$  is set to 4 as person images of identity and  $P$  is set to 8 as pseudo person identities. The synthetic person image number for each input image  $S$  is set to 4. So we process 160 images per mini-batch. We set the weight factor of loss  $\alpha$  as 0.3. We set

Table 1: Comparison on PRCC and VC-Clothes datasets. The R1 is Rank-1 CMC accuracies (%). The mAP denotes mean Average Precision score (%).

Method	PRCC				VC-Clothes			
	Clothing Change		Same Clothing		Clothing Change		Same Clothing	
	R1	mAP	R1	mAP	R1	mAP	R1	mAP
LOMO(Liao et al. 2015) + KISSME(Koestinger et al. 2012)	18.55	-	47.40	-	-	-	-	-
LOMO(Liao et al. 2015) + XQDA(Liao et al. 2015)	14.53	-	29.41	-	34.5	30.9	86.2	83.3
PCB(Sun et al. 2018)	41.8	38.7	86.88	-	62.0	62.2	94.7	94.3
RGA-SC(Zhang et al. 2020)	42.3	-	98.4	-	71.1	67.4	95.4	94.8
MGN(Wang et al. 2018a)	33.8	35.9	99.5	98.4	-	-	-	-
LTCC(Qian et al. 2020)	34.38	-	64.2	-	-	-	-	-
FSAM(Hong et al. 2021)	54.5	-	98.8	-	78.6	78.9	94.7	94.8
SGPS(Shu et al. 2021)	65.8	61.2	99.5	96.7	-	-	-	-
Sync-Person-Cloud	43.7	39.8	87.4	82.1	67.4	62.5	91.9	89.3

the momentum for update the memory instance  $m$  as 0.3.

We use Adam optimizer and set both the weight decay factor and weight decay bias factor as 0.0005. The base learning rate is 0.00035. We use a linear warming up strategy for adjustment of learning rate at train stage. For the first  $E_{warmup}$  epoch with start learning rate  $R_{start}$ , the learning rate will linearly increase from  $\frac{R_{start}}{E_{warmup}}$  to  $R_{start}$ . We set warm-up iteration number  $E_{warmup}$  as 20 in our experiments. The total training epoch number is 120. We set the maximum distance  $\varepsilon$  between two samples as 0.4 and the minimal number of neighbors in a core point  $M$  as 4 for our clustering method DBScan hyperparameters.

## 4.2 Datasets and Evaluation Protocol

We mainly evaluated our method on two cloth changing ReID datasets: PRCC (Yang, Wu, and Zheng 2019) and VC-Clothes (Wan et al. 2020).

PRCC is named Person Re-id under the moderate Clothing Change dataset. It was collected for the task of cloth-changing person re-ID. PRCC consists of 221 identities captured by three camera views. VC-Clothes is a synthetic dataset rendered by the GTA5 game engine, which contains 19060 images of 512 identities captured from 4 cameras.

For evaluation protocol, we adopted the mean average precision (mAP) and ard Cumulative Matching Characteristics (CMC) rank-k accuracy. For both cloth-changing datasets PRCC and VC-Clothes, we followed their evaluation protocols and evaluated the performance. For PRCC, we used single-shot matching by randomly choosing one image of each identity as the gallery. The cloth-changing setting in PRCC means there are all clothing change samples in the test set. For VC-Clothes, we used multi-shot matching and the clothing change setting is the same as that of PRCC. We also do the experiments on both datasets under the same clothing settings, whose test sets are all cloth-consistent samples in the test set.

## 4.3 Comparison With the State-of-The-Art

As there is no existing unsupervised clothing change person ReID method, we compare our method with the state-of-the-art supervised clothing change person ReID method. As

shown in Table 1, we can see that our method is not the highest solution overall methods. The reason is that although we use person augmentation information and a strong unsupervised deep ReID pipeline, our model still lacks some supervised information to converge the ReID backbone. Through self identity constrain loss for synthetic clothing change person image feature and using a clustering algorithm to get pseudo labels, we can get some identity information from the dataset. However, the pseudo label is inaccurate and the person number keeps change so that we can't use classification loss. The synthetic clothing change image is generated from a pretrained *PISE* module, whose image information is from other texture style transfer datasets. Hence, the quality of the supervised information restricts our model's ability.

However, our method can perform as well as some supervised person ReID model, which is not design for clothing change scenarios. As shown in the table 1, our method have higher Rank 1 accuracy and mAP than PCB (Sun et al. 2018), RGA-SC (Zhang et al. 2020) and LOMO (Liao et al. 2015). Hence, our method is effective for unsupervised clothing change ReID.

## 4.4 Ablation Study

**Component Effectiveness** In this section, we study the effectiveness of key components of our proposed method. We take PRCC dataset under clothing change settings as an example. The baseline is a pure unsupervised person ReID pipeline. The components include  $C_a$ ,  $C_i$  and  $C_s$ .  $C_a$  is the *PISE* person clothing change image augmentation module,  $C_i$  is the self identity constrain loss and  $C_s$  is the cluster average and hardest sample operation. Because the  $C_i$  must be based on  $C_a$ , we need to at least use both components when we want to analyze the effectiveness of  $C_i$ . The results of our proposed different components' effectiveness are shown in Table 2.

As shown in Table 2, our proposed model with all components significantly outperformed the baseline model. The baseline gets 29.6% R1 accuracy, which is much lower than the most of state of the art method. By using  $C_a$ , we can get much more information from the augmented clothing change person images. Through training these images, the

Table 2: Self comparison on PRCC dataset.

Method	Component			PRCC	
	$C_a$	$C_i$	$C_s$	R1	mAP
Baseline				29.6	27.4
Baseline	✓			30.3	27.9
Baseline			✓	32.4	30.8
Baseline	✓		✓	35.1	33.3
Baseline	✓	✓		37.2	35.3
Sync-Person-Cloud	✓	✓	✓	43.7	39.8

model can improve 0.7% R1 accuracy, which is not so significant. The reason for the low improvement is that although we use the augmentation module, the identity information is still not be constrained and with more images information it is hard for the model to converge. By using  $C_s$ , we can get 2.8% R1 accuracy improvement. The hardest and average sampling can help the model with better and faster convergence. The average sampling can help the model learn more global information in the dataset and the hardest sampling can help the model learn from an extreme instance. Hence, by combining  $C_a$  and  $C_s$  together, we can get 35.1% in R1 accuracy. Through using  $C_i$  to constrain the synthetic person image features generated from the same original input person image, the model can get 37.2% R1 accuracy. This significant improvement shows that the augmentation images have abundant person identity information for model disentanglement between people’s clothing and identity, which helps our model to adapt the clothing change person ReID scenario. Finally, our method with all components can reach the highest R1 accuracy 43.7%, which means that the  $C_a$ ,  $C_i$  and  $C_s$  can work well corporately.

**Sample Method** In this section, we want to discuss the effectiveness of our sampling method. We take PRCC dataset under clothing change settings as an example.

Table 3: Sampling method comparison on PRCC dataset.

Sampling Method	PRCC	
	R1	mAP
No Sample	37.2	35.3
Average Sample	36.1	34.7
Hardest Sample	41.2	37.4
Both	43.7	39.8

The comparison results are shown in Table 3. All the settings are based on our model with image augmentation and self identity constrain. The first setting is that we don’t use sampling in our contrast module, which means the query features and memory need to update one by one. In this case, the feature memory is not a single instance for each identity. It will record multiple instances in the memory to decrease the update frequency for each instance. It can achieve 37.2% in Rank1 accuracy. Using the average sampling method decreases the accuracy by 1.1% than first settings. The reason is mainly that although we use the average sample to reduce the memory load and utilize the global information

of the same pseudo person, the model is harder to converge than use all the instances one by one. Another reason is that the pseudo label is not stable for update global information, which also causes low performance. By using the hardest sampling method, we can get 41.2% Rank1 accuracy. The hardest sampling can help the model better converge and learn from the extreme image features. By using both average and hardest sampling, our model can get the highest Rank1 accuracy 43.7%. In this situation, using global information is not the obstruction of the model convergence with the help from the hardest sampling. The hardest sampling will lead the gradient to the extreme instance and average sampling will help the model keep the global information of all images (including the synthetic clothing change images).

**DBScan Hyper-parameters** In the DBScan clustering algorithm,  $\epsilon$  is the maximum distance between two samples for one to be considered as in the neighborhood of the other. It greatly affects the performance of clustering by deciding the final number of clusters (person pseudo identity numbers in our case).

When  $\epsilon$  is too small, the cluster with a small density will be divided into multiple clusters with similar properties. However, when  $\epsilon$  is too large, clusters with a closer distance and a larger density will be merged into one cluster. In the case of high-dimensional data in the person ReID problem, it is more difficult to select the  $\epsilon$  value due to the curse of dimensionality. We analyze  $\epsilon$  influence on the PRCC dataset under clothing change settings using our whole model.

Table 4: Analysis of  $\epsilon$  value on PRCC dataset.

$\epsilon$ Value	PRCC	
	R1	mAP
0.2	38.4	33.1
0.3	41.2	36.5
0.4	43.7	39.8
0.5	40.8	35.9
0.6	40.2	35.8
0.7	40.4	34.1

As shown in the Table 4, we can see that our method works best when  $\epsilon$  equals 0.4.

## 5 Conclusion

In this paper, to solve the lack of person identity label and clothing change problem in person ReID, we propose an unsupervised clothing change person ReID model called Sync-Person-Cloud. To our best knowledge, we are the first to use unsupervised learning in the clothing change ReID problem. To improve the ability of extraction clothing change invariant information of our model, we propose a self identity constrain for synthetic clothing change person image and a hardest and average sampling method for cluster contrast. Experiments show the performance of our model compared with the state-of-the-art supervised clothing change person ReID methods.

## References

- Barbosa, I. B.; Cristani, M.; Del Bue, A.; Bazzani, L.; and Murino, V. 2012. Re-identification with rgb-d sensors. In *European Conference on Computer Vision*, 433–442. Springer.
- Chang, X.; Hospedales, T. M.; and Xiang, T. 2018. Multi-level factorisation net for person re-identification. In *CVPR*, 2109–2118.
- Chen, W.; Chen, X.; Zhang, J.; and Huang, K. 2017. Beyond triplet loss: a deep quadruplet network for person re-identification. In *CVPR*, 403–412.
- Concha, O. P.; Da Xu, R. Y.; Moghaddam, Z.; and Piccardi, M. 2011. HMM-MIO: an enhanced hidden Markov model for action recognition. In *CVPR 2011 WORKSHOPS*, 62–69. IEEE.
- Dai, Z.; Wang, G.; Yuan, W.; Zhu, S.; and Tan, P. 2021. Cluster Contrast for Unsupervised Person Re-Identification. *arXiv preprint arXiv:2103.11568*.
- Day, W. H.; and Edelsbrunner, H. 1984. Efficient algorithms for agglomerative hierarchical clustering methods. *Journal of classification*, 1(1): 7–24.
- Deng, J.; Dong, W.; Socher, R.; Li, L.-J.; Li, K.; and Fei-Fei, L. 2009. Imagenet: A large-scale hierarchical image database. In *2009 IEEE conference on computer vision and pattern recognition*, 248–255. Ieee.
- Deng, W.; Zheng, L.; Ye, Q.; Kang, G.; Yang, Y.; and Jiao, J. 2018. Image-image domain adaptation with preserved self-similarity and domain-dissimilarity for person re-identification. In *Proceedings of the IEEE conference on computer vision and pattern recognition*, 994–1003.
- Ding, S.; Lin, L.; Wang, G.; and Chao, H. 2015. Deep feature learning with relative distance comparison for person re-identification. *Pattern Recognition*, 48(10): 2993–3003.
- Ester, M.; Kriegel, H.-P.; Sander, J.; Xu, X.; et al. 1996. A density-based algorithm for discovering clusters in large spatial databases with noise. In *kdd*, volume 96, 226–231.
- Fan, H.; Zheng, L.; Yan, C.; and Yang, Y. 2018. Unsupervised person re-identification: Clustering and fine-tuning. *ACM Transactions on Multimedia Computing, Communications, and Applications (TOMM)*, 14(4): 1–18.
- Fu, Y.; Wei, Y.; Wang, G.; Zhou, Y.; Shi, H.; and Huang, T. S. 2019. Self-similarity grouping: A simple unsupervised cross domain adaptation approach for person re-identification. In *Proceedings of the IEEE/CVF International Conference on Computer Vision*, 6112–6121.
- He, K.; Zhang, X.; Ren, S.; and Sun, J. 2016. Deep residual learning for image recognition. In *CVPR*, 770–778.
- Hermans, A.; Beyer, L.; and Leibe, B. 2017. In defense of the triplet loss for person re-identification. *arXiv preprint arXiv:1703.07737*.
- Hong, P.; Wu, T.; Wu, A.; Han, X.; and Zheng, W.-S. 2021. Fine-Grained Shape-Appearance Mutual Learning for Cloth-Changing Person Re-Identification. In *Proceedings of the IEEE/CVF Conference on Computer Vision and Pattern Recognition*, 10513–10522.
- Hou, R.; Ma, B.; Chang, H.; Gu, X.; Shan, S.; and Chen, X. 2019. VRSTC: Occlusion-Free Video Person Re-Identification. In *CVPR*, 7183–7192.
- Koestinger, M.; Hirzer, M.; Wohlhart, P.; Roth, P. M.; and Bischof, H. 2012. Large scale metric learning from equivalence constraints. In *2012 IEEE conference on computer vision and pattern recognition*, 2288–2295. IEEE.
- Li, Y.-J.; Chen, Y.-C.; Lin, Y.-Y.; Du, X.; and Wang, Y.-C. F. 2019. Recover and identify: A generative dual model for cross-resolution person re-identification. In *ICCV*, 8090–8099.
- Liao, S.; Hu, Y.; Zhu, X.; and Li, S. Z. 2015. Person re-identification by local maximal occurrence representation and metric learning. In *CVPR*, 2197–2206.
- Lin, S.; Li, H.; Li, C.-T.; and Kot, A. C. 2018. Multi-task mid-level feature alignment network for unsupervised cross-dataset person re-identification. *arXiv preprint arXiv:1807.01440*.
- Lin, Y.; Dong, X.; Zheng, L.; Yan, Y.; and Yang, Y. 2019. A bottom-up clustering approach to unsupervised person re-identification. In *Proceedings of the AAAI Conference on Artificial Intelligence*, volume 33, 8738–8745.
- Liu, J.; Ni, B.; Yan, Y.; Zhou, P.; Cheng, S.; and Hu, J. 2018. Pose transferrable person re-identification. In *Proceedings of the IEEE Conference on Computer Vision and Pattern Recognition*, 4099–4108.
- MacQueen, J.; et al. 1967. Some methods for classification and analysis of multivariate observations. In *Proceedings of the fifth Berkeley symposium on mathematical statistics and probability*, volume 1, 281–297. Oakland, CA, USA.
- Oord, A. v. d.; Li, Y.; and Vinyals, O. 2018. Representation learning with contrastive predictive coding. *arXiv preprint arXiv:1807.03748*.
- Paszke, A.; Gross, S.; Massa, F.; Lerer, A.; Bradbury, J.; Chanan, G.; Killeen, T.; Lin, Z.; Gimelshein, N.; Antiga, L.; et al. 2019. Pytorch: An imperative style, high-performance deep learning library. In *NeurIPS*, 8026–8037.
- Qian, X.; Fu, Y.; Xiang, T.; Wang, W.; Qiu, J.; Wu, Y.; Jiang, Y.-G.; and Xue, X. 2018. Pose-normalized image generation for person re-identification. In *ECCV*, 650–667.
- Qian, X.; Wang, W.; Zhang, L.; Zhu, F.; Fu, Y.; Xiang, T.; Jiang, Y.-G.; and Xue, X. 2020. Long-term cloth-changing person re-identification. In *Proceedings of the Asian Conference on Computer Vision*.
- Shu, X.; Li, G.; Wang, X.; Ruan, W.; and Tian, Q. 2021. Semantic-guided Pixel Sampling for Cloth-Changing Person Re-identification. *IEEE Signal Processing Letters*.
- Si, J.; Zhang, H.; Li, C.-G.; Kuen, J.; Kong, X.; Kot, A. C.; and Wang, G. 2018. Dual attention matching network for context-aware feature sequence based person re-identification. In *CVPR*, 5363–5372.
- Song, C.; Huang, Y.; Ouyang, W.; and Wang, L. 2018. Mask-guided contrastive attention model for person re-identification. In *Proceedings of the IEEE conference on computer vision and pattern recognition*, 1179–1188.



- Sun, Y.; Zheng, L.; Yang, Y.; Tian, Q.; and Wang, S. 2018. Beyond part models: Person retrieval with refined part pooling (and a strong convolutional baseline). In *ECCV*, 480–496.
- Wan, F.; Wu, Y.; Qian, X.; and Fu, Y. 2020. When Person Re-identification Meets Changing Clothes. *arXiv preprint arXiv:2003.04070*.
- Wang, G.; Lai, J.; Huang, P.; and Xie, X. 2019a. Spatial-temporal person re-identification. In *AAAI*, volume 33, 8933–8940.
- Wang, G.; Yuan, Y.; Chen, X.; Li, J.; and Zhou, X. 2018a. Learning discriminative features with multiple granularities for person re-identification. In *ACMMM*, 274–282. ACM.
- Wang, G.; Zhang, T.; Cheng, J.; Liu, S.; Yang, Y.; and Hou, Z. 2019b. RGB-Infrared Cross-Modality Person Re-Identification via Joint Pixel and Feature Alignment. In *ICCV*, 3623–3632.
- Wang, J.; Zhu, X.; Gong, S.; and Li, W. 2018b. Transferable joint attribute-identity deep learning for unsupervised person re-identification. In *Proceedings of the IEEE conference on computer vision and pattern recognition*, 2275–2284.
- Wang, Z.; Ye, M.; Yang, F.; Bai, X.; and Satoh, S. 2018c. Cascaded SR-GAN for scale-adaptive low resolution person re-identification. In *IJCAI*, volume 1, 4.
- Wu, A.; Zheng, W.-S.; Yu, H.-X.; Gong, S.; and Lai, J. 2017. Rgb-infrared cross-modality person re-identification. In *ICCV*, 5380–5389.
- Wu, Z.; Xiong, Y.; Yu, S. X.; and Lin, D. 2018. Unsupervised feature learning via non-parametric instance discrimination. In *Proceedings of the IEEE conference on computer vision and pattern recognition*, 3733–3742.
- Xue, J.; Meng, Z.; Katipally, K.; Wang, H.; and van Zon, K. 2018. Clothing change aware person identification. In *Proceedings of the IEEE Conference on Computer Vision and Pattern Recognition Workshops*, 2112–2120.
- Yang, Q.; Wu, A.; and Zheng, W.-S. 2019. Person re-identification by contour sketch under moderate clothing change. *IEEE Transactions on Pattern Analysis and Machine Intelligence*.
- Yang, X.; Wang, M.; and Tao, D. 2017. Person re-identification with metric learning using privileged information. *IEEE Transactions on Image Processing*, 27(2): 791–805.
- Ye, M.; Shen, J.; Lin, G.; Xiang, T.; Shao, L.; and Hoi, S. C. 2021. Deep learning for person re-identification: A survey and outlook. *IEEE Transactions on Pattern Analysis and Machine Intelligence*.
- Yi, D.; Lei, Z.; Liao, S.; and Li, S. Z. 2014. Deep metric learning for person re-identification. In *2014 22nd International Conference on Pattern Recognition*, 34–39. IEEE.
- Yu, H.-X.; Zheng, W.-S.; Wu, A.; Guo, X.; Gong, S.; and Lai, J.-H. 2019. Unsupervised person re-identification by soft multilabel learning. In *Proceedings of the IEEE/CVF Conference on Computer Vision and Pattern Recognition*, 2148–2157.
- Zhang, J.; Li, K.; Lai, Y.-K.; and Yang, J. 2021a. PISE: Person Image Synthesis and Editing With Decoupled GAN. In *Proceedings of the IEEE/CVF Conference on Computer Vision and Pattern Recognition (CVPR)*, 7982–7990.
- Zhang, Z.; Da Xu, R. Y.; Jiang, S.; Li, Y.; Huang, C.; and Deng, C. 2020. Illumination Adaptive Person Reid Based on Teacher-Student Model and Adversarial Training. In *ICIP*, 2321–2325.
- Zhang, Z.; Jiang, S.; Huang, C.; Li, Y.; and Da Xu, R. Y. 2021b. RGB-IR cross-modality person ReID based on teacher-student GAN model. *Pattern Recognition Letters*, 150: 155–161.
- Zhang, Z.; Lan, C.; Zeng, W.; Jin, X.; and Chen, Z. 2020. Relation-aware global attention for person re-identification. In *Proceedings of the IEEE/CVF conference on computer vision and pattern recognition*, 3186–3195.
- Zheng, Z.; Zheng, L.; and Yang, Y. 2017. Unlabeled Samples Generated by GAN Improve the Person Re-identification Baseline in vitro. In *ICCV*.
- Zhong, Z.; Zheng, L.; Zheng, Z.; Li, S.; and Yang, Y. 2018. Camera style adaptation for person re-identification. In *Proceedings of the IEEE conference on computer vision and pattern recognition*, 5157–5166.